

Document downloaded from:

<http://hdl.handle.net/10251/140926>

This paper must be cited as:

Menzel, C.; González Martínez, MC.; Chiralt, A.; Vilaplana, F. (15-0). Antioxidant starch films containing sunflower hull extracts. *Carbohydrate Polymers*. 214:142-151.
<https://doi.org/10.1016/j.carbpol.2019.03.022>



The final publication is available at

<https://doi.org/10.1016/j.carbpol.2019.03.022>

Copyright Elsevier

Additional Information

1 **Antioxidant starch films containing sunflower hull extracts**

2

3 *Carolin Menzel*^{1,2*}, *Chelo González-Martínez*², *Amparo Chiralt*², *Francisco Vilaplana*¹

4

5 ¹Division of Glycoscience, Department of Chemistry, School of Engineering Sciences in
6 Chemistry, Chemistry, Biotechnology and Health, KTH Royal Institute of Technology,
7 AlbaNova University Centre, Stockholm, Sweden

8 ²Departamento de Tecnología de Alimentos, Instituto de Ingeniería de Alimentos para el
9 Desarrollo, Universitat Politècnica de Valencia, Spain

10

11 *Corresponding author:

12 Carolin Menzel, E-mail: cmenzel@kth.se, tel.: +46 87909939, postal address: KTH Royal
13 Institute of Technology, Roslagstullbacken 21, Plan 2, SE-10044 Stockholm, Sweden

14

15 E-mail addresses of other authors:

16 Chelo González-Martínez: cgonza@tal.upv.es

17 Amparo Chiralt: dchiralt@tal.upv.es

18 Francisco Vilaplana: franvila@kth.se

19 **ABSTRACT**

20 This study explores the preparation of antioxidant starch food packaging materials by the
21 incorporation of valuable phenolic compounds extracted from sunflower hulls, which are an
22 abundant by-product from food industry. The phenolic compounds were extracted from
23 sunflower hulls with aqueous methanol and embedded into potato starch films obtained by
24 melt blending and compression molding. Their effect on starch films was investigated in
25 terms of antioxidant activity, optical, thermal, mechanical, and barrier properties. The changes
26 in the starch molecular structure due to the film processing conditions were also studied. The
27 results showed that starch molecular structure was affected during thermal processing
28 resulting in a decrease in weight-average molecular weight \bar{M}_w of native starch 9.1×10^6 Da
29 $10^6 \times 3.6 - 1.1$ Da in starch films, smaller amylopectin molecules and shorter amylose branches
30 as observed after isoamylase debranching. Already 1-2% of extracts were sufficient to
31 produce active starch films with high antioxidant capacity without the loss of barrier
32 properties. High amounts (4-6%) of extract showed the highest antioxidant activity, the lowest
33 oxygen and water vapor permeability and high stiffness and poor extensibility. The phenolic
34 extracts affected predominantly the mechanical properties, whereas other changes could
35 mainly be correlated to the lower glycerol content which was partially substituted by the
36 extract.

37

38 **KEYWORDS:** renewable packaging, physical properties, antimicrobial activity, molecular
39 weight, DPPH, chlorogenic acid

40 1. INTRODUCTION

41 There is an increasing interest to exploit by-products from food industries as matrices and
42 additives in packaging materials contributing to the material and process sustainability
43 towards a circular bio-based economy. An illustrative example of the potential of such by-
44 products are sunflower hulls. In 2016, the world production of sunflower seed was estimated
45 to 49.9 million tons, with Ukraine and Russia as major producers counting for 27% and 22%,
46 respectively (FAOSTAT, 2016). Sunflower hulls are a by-product from sunflower seed
47 production and exhibit very low nutritional value for human and animal nutrition due to their
48 low digestibility. The hull represents between 20-30% of the sunflower seed and is often
49 removed before oil extraction or snack processing. Hulls are mainly composed of
50 carbohydrates (of which are 40-50% cellulose) and low amounts of lipids and proteins
51 (Cancalon, 1971). However, sunflower hulls have also a great antioxidant activity due to a
52 high value of total phenolic compounds (Velioglu, Mazza, Gao, & Oomah, 1998) that could
53 have potential for obtaining antioxidant extracts. De Leonardis, Macciola, and Di Domenico
54 (2005) extracted an antioxidant product from sunflower hulls that was reported to be
55 economically suitable. Furthermore, there has been a patent on a natural red sunflower
56 anthocyanin colorant with naturally stabilized color qualities as coloring agent in food
57 products, cosmetics and pharmaceuticals (Fox, 2000).

58 In the framework of the relatively recent concept of active and intelligent packaging, the
59 incorporation of antioxidants or antimicrobials to packaging materials is useful to extend the
60 shelf-life and improve food safety or sensory properties (Valdés, Mellinas, Ramos, Garrigós,
61 & Jiménez, 2014). Active packaging systems can either deliver a compound into the packaged
62 food and into the headspace or remove undesired compounds from the product and its
63 environment. Most developments aim to directly incorporate active components into the
64 polymer matrix of the packaging but at the same time maintaining or improving the barrier
65 and mechanical properties of the initial material. Natural compounds with antioxidant

66 properties currently show a significant interest and can potentially be used in food packaging
67 to replace synthetic antioxidants, as they can be biologically degradable and are normally
68 considered as safe migrants (Dainelli, Gontard, Spyropoulos, Zondervan-van den Beuken, &
69 Tობback, 2008). For instance, the addition of antioxidants such as α -tocopherol or citric acid
70 into edible starch-chitosan blends resulted in good antioxidant capacity of the films but also
71 good barrier properties (Bonilla, Talón, Atarés, Vargas, & Chiralt, 2013). The incorporation
72 of plant essential oils has been shown to enhance mechanical and barrier properties of starch
73 films (Ghasemlou et al., 2013) but also to increase the antioxidant capacity of films and their
74 antimicrobial properties (Oriani, Molina, Chiumarelli, Pastore, & Hubinger, 2014). Likewise,
75 starch is a very promising biopolymer for the production of packaging materials since it is not
76 only renewable but also biodegradable and available with high purity at low cost (Jiménez,
77 Fabra, Talens, & Chiralt, 2012; Versino, Lopez, Garcia, & Zaritzky, 2016). Starch consists of
78 two main polymers, amylose and amylopectin, with distinct branching structure and
79 physicochemical properties. Amylose is considered as an almost linear polymer consisting of
80 linear chains of α -(1 \rightarrow 4)-linked glucose units with very few α -(1 \rightarrow 6) glycosidic bonds at the
81 branching points, and a molecular weight of about 10^6 Da. Amylopectin, on the other hand, is
82 a highly branched macromolecule comprising of many α -(1 \rightarrow 4)-linked glucose short
83 elongated chains, branched by α -(1 \rightarrow 6) glycosidic bonds, with a much larger molecular
84 weight of about 10^8 Da. Native starch exists as a granular structure and can be thermo-
85 processed into a continuous phase, i.e., thermoplastic starch, which forms films with excellent
86 oxygen barrier properties. However, starch films still demonstrate problems such as
87 brittleness in the absence of a plasticizer and a very hydrophilic character, which results in
88 water sensitivity and poor moisture barrier properties.

89 In this study the suitability of sunflower hulls for the extraction of antioxidants was
90 investigated and their potential use as additive in starch films to produce renewable food
91 packaging materials was demonstrated as a proof of concept. Therefore, the extraction process

92 of an antioxidant fraction was optimized and the extract was characterized in terms of its total
93 phenolic content, antioxidant capacity, antimicrobial activity and phenolic acid composition.
94 The final phenolic extract was included into compression molded starch films which were
95 analyzed in terms of their in-vitro antioxidant capacity, appearance, tensile and barrier
96 properties. The changes in the molecular structure of starch during the film production were
97 assessed in terms of molar mass and branch chain-length distribution of the amylopectin and
98 amylose components.

99

100 **2. MATERIALS AND METHODS**

101 *2.1 Materials*

102 Sunflower hulls were kindly supplied by Grefusa (Alzira, Spain) as waste by-product of the
103 snack sunflower seed production. Potato starch was supplied by Roquette (France) with an
104 amylose content of 27%, calculated as the area under the curve of the branch chain-length
105 distributions of debranched native potato starch for DP above 200 units, according to
106 Vilaplana, Hasjim, and Gilbert (2012).

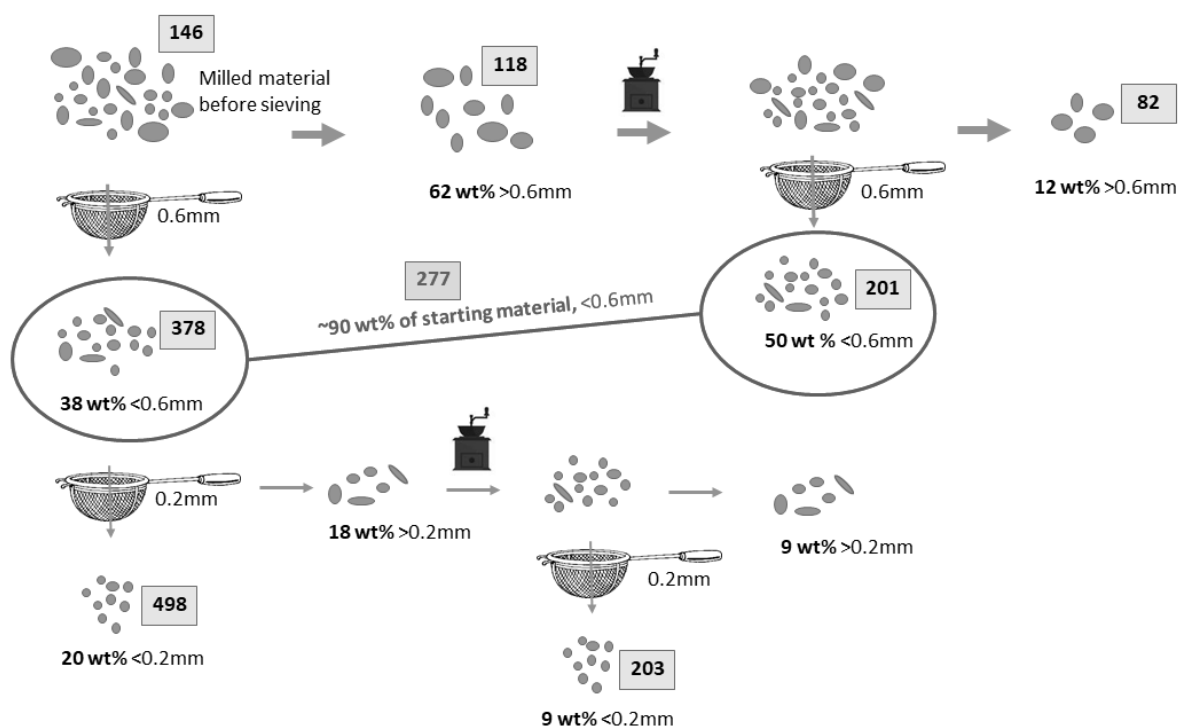
107 Glycerol, sodium carbonate, methanol and ethanol were purchased from PanReac Quimica
108 S.L.U. (Castellar del Vallés, Barcelona, Spain). Gallic acid, caffeic acid, pyrogallol, ferulic
109 acid, chlorogenic acid, 2,2-Diphenyl-1-picrylhydrazyl (DPPH) and Folin-Ciocalteu reagent
110 (2N) were purchased from Sigma-Aldrich (Saint Louis, USA). All other reagents and solvents
111 were of analytical grade. Phosphate buffered saline, tryptone soy broth, tryptone soy agar and
112 thiazolyl blue tetrazolium bromide (MTT) reagent were purchased by Scharlab (Barcelona,
113 Spain). *Escherichia coli* (CECT 101) y *Listeria innocua* were obtained from the Spanish Type
114 Collection (CECT, University de Valencia, Spain).

115

116 *2.2 Extraction of phenolics from sunflower hulls and evaluation of their activity*

117 *2.2.1 Extraction of total phenolics from sunflower hull residue*

118 Sunflower hulls were washed with water and residues of kernels, sand and other impurities
 119 were allowed to settle down. Hulls were very light and were swimming on the water surface,
 120 hence, hulls were easily skimmed off and dried at 40 °C overnight. The hulls were milled
 121 using a Moulinex mixer. The milling process was optimized using several sieving (<0.6mm
 122 and <0.2mm) and milling steps (up to 3 times) by measuring total phenolic content using
 123 Folin-reagent in the different fractions (schematic Fig. 1) extracted with 80% aqueous MeOH,
 124 stirred for 30 min at room temperature, by using a 1:20 hull:solvent ratio. After optimization
 125 of the milling process, the extraction process was further optimized.



126
 127 **Figure 1.** Schematic milling and sieving process, with weight percentage (bold numbers with
 128 particle size) based on 100% starting material that passed the sieve of 0.6 mm or 0.2 mm after
 129 continuous milling. Joined material with particle size <0.6mm (red marked) was used for all
 130 further extractions. Numbers in casket are total phenolic contents expressed as mg GAE/ 100g
 131 DM sample).

132
 133 The extraction of phenolic compounds was conducted using either 80% aqueous MeOH or
 134 80% aqueous EtOH at either 1:10 or 1:20 hull:solvent ratio for 30 min or 1 h. Subsequently,
 135 the organic solvent was evaporated at 35 °C under vacuum and the residual extract was

136 lyophilized. The weight of the dry residue was determined. All determinations were done in
137 triplicate.

138

139 *2.2.2 Determination of total phenolic content*

140 Total phenolic content was determined using Folin-Ciocalteu reagent. In brief, 0.5 ml sample
141 extract and 6 ml distilled water were first mixed in a glass tube and then 0.5 ml Folin reagent
142 (2N) were added. After one minute, 1.5 ml sodium carbonate solution (20%, w/v) was added
143 and the mixture was filled up to 10 ml with distilled water and incubated for 2 h at room
144 temperature in the dark. The absorbance was measured spectrophotometrically at 725 nm
145 using a UV-Vis spectrophotometer (Evolution 201, Thermo Scientific) against a solvent blank
146 of methanol. A gallic acid solution was used as a standard for calibration and total phenolic
147 content was expressed as mg of gallic acid equivalents (GAE) /100 g of dry sunflower hulls.
148 All determinations were performed in triplicates.

149

150 *2.2.3 Evaluation of antioxidant capacity using DPPH* assay*

151 The antioxidant capacity was evaluated by the DPPH* assay according to Brand-Williams,
152 Cuvelier, and Berset (1995) with small modifications. In brief, a solution of 0.06 mM DPPH
153 in methanol was added to 4 ml total volume in a cuvette to different amounts of the
154 methanolic and ethanolic fraction extracted from the sunflower hulls (0.10, 0.15, 0.20, 0.25,
155 0.30, 0.35 ml). A blank sample was prepared using the same volumes of ethanolic or
156 methanolic solvent. Solutions were kept in the dark for 4 h at room temperature. A reaction
157 time of 4 h was necessary until a stable absorbance was reached. The resulting absorbance
158 was measured at 515 nm using a spectrophotometer (Evolution 201, Thermo Scientific). All
159 determinations were done in triplicate and results were expressed as amount necessary to
160 decrease the initial DPPH* concentration by 50% (Efficient concentration=EC₅₀ in mg dry
161 material/mg DPPH* (Brand-Williams et al., 1995).

162

163 *2.2.4 Identification and quantification of phenolic acids using HPLC-DAD*

164 Phenolic acids in the extracts were determined according to Szydłowska-Czerniak,
165 Trokowski, and Szlyk (2011) using a Waters HPLC-DAD system (Waters 2695 separation
166 module, Waters 2996 photodiode array detector) equipped with a Waters Empower Data
167 Chromatography Software. A RP-C18 column (Brisa LC2 C18 5 µm particle size,
168 250 mm x 4.6 mm i.D., Teknokroma Analytítica, Spain) with a C18 guard column from
169 Phenomenex (3.2-8.0mm i.D.) was used for separation and operated at 25 °C and 1 mL/ min
170 flow rate. The mobile phase consisted of 2% (v/v) acetic acid in water (eluent A) and 100%
171 methanol (eluent B). The gradient was as follows: 100-75% A (11 min), 71.25% A (4 min),
172 64% A (10 min), 55% A (10 min), 35% A (3 min), 100% A (3 min) and 100% A (4 min).
173 The column was washed with 100% B for 10 min and equilibrated to the starting conditions
174 for 5 min before next injection. The total run time was 60 min and injection volume of each
175 sample and calibration standard was 20 µL. Calibration was carried out between 0.5 and
176 100 mg/ L of caffeic acid, chlorogenic acid, gallic acid, pyrogalllic acid and ferulic acid and
177 UV/Vis spectra between 210-400nm were recorded at a spectral acquisition rate of
178 1.25 scans/ s. Individual compounds were quantified using a calibration curve of the
179 corresponding standard compound at either 325 nm or 270 nm. All determinations were
180 performed in triplicates.

181

182 *2.2.5 Antimicrobial activity of sunflower hull extracts*

183 Antimicrobial activity of sunflower hull extracts were tested against *E. coli* (CECT 101) and
184 *Listeria innocua* (CECT 910) using the MTT assay on a 96-well microtiter plates according
185 to Houdkova, Rondevaldova, Doskocil, and Kokoska (2017). The MTT assay is a
186 colorimetric assay for assessing cell metabolic activity. NAD(P)H-dependent cellular
187 oxidoreductase enzymes may, under defined conditions, reflect the number of viable cells

188 present. These enzymes are capable of reducing the tetrazolium dye MTT to its insoluble
189 formazan, which has a purple color and can be detected visually.

190 The bacterial strains were grown in tryptone soy buffer and diluted to a working solution of
191 10^5 colony forming unit (CFU). A MTT reagent was freshly prepared (5 mg/ml) and freeze-
192 dried phenolic extracts from sunflower hulls were dissolved in the tryptone soy buffer
193 (100 mg/ml). The minimum inhibitory concentration (MIC) determination of both bacteria
194 strains were performed in 96-well plates with the following scheme; for each bacteria strain
195 100 μ l of the 10^5 CFU dispersion was added to the wells and 10, 20, 30, 40, 50, 60, 70, 80, 90
196 or 100 μ l sample solution was added together with the appropriate amount of tryptone soy
197 buffer to give a final volume of 200 μ l in each well. The plate was incubated at 37 °C for
198 24 h. Afterwards 10 μ l MTT solution was added to each well and incubated again for 4 h
199 more at 37 °C. Finally the growth was checked visually by observing the change of colour
200 since alive bacteria has the capacity to metabolize the MTT reagent and form a purple
201 complex. The amount of sample that showed no purple colour formation indicates the MIC.

202

203 *2.3 Preparation and characterization of starch films with bioactive properties*

204 *2.3.1 Starch film preparation using melt blending and compression molding*

205 Native potato starch was blended with glycerol (0.25 g/g starch), using 40 g starch and 10 g
206 glycerol (CS_10G). Glycerol was partially substituted by four different amounts of phenolic
207 extract, 0.5 g, 1 g, 2 g and 3 g which resulted in 1, 2, 4 and 6 wt% of extract within the film
208 forming formulation. Furthermore, one starch formulation with 40 g starch and 7 g glycerol
209 (CS_7G) was prepared for comparison purposes. Table 3 shows the film composition and
210 sample codes. The blends were introduced into an internal mixer (Haake PolyLab QC,
211 Thermo Fisher Scientific, Germany) and homogenized at 160 °C for 7 min. The antioxidant
212 extract (AOE) was added seven minutes after the starch had been blended in the internal
213 mixer with glycerol and mixing continued 2 min more. The mixer chambers were preheated at

214 160 °C with rotors operating at 50 rpm. The optimum conditions to process potato starch with
215 glycerol in the internal mixer were pre-determined using different mixing times and
216 temperatures and monitoring the evolution of torque during the mixing.

217 The processed melts were grinded and equilibrated at 53% relative humidity (RH) at 25 °C
218 for 7 days and afterwards films of about 200 µm thickness were produced by compression
219 molding using Teflon molds of about 20 cm diameter. About 4 g of starch melt was
220 introduced between two metal plates and preheated at 160 °C for 4 min without applying
221 pressure. During the following 8 min heating cycle, the pressure was increased from 30 bar
222 (2 min) to 130 bar (6 min) and afterwards a fast cooling (3 min) was applied to reduce the
223 temperature to about 70 °C. The films were conditioned at 53% RH for 7 days at room
224 temperature in a sealed chamber containing an oversaturated solution of magnesium nitrate.
225 RH was measured by a digital RH-meter. Thickness of the conditioned films was measured in
226 at least six random points of each sample using a digital electronic micrometer with an
227 accuracy of 0.001mm (Palmer model COMECTA, Barcelona). Digital pictures of the films
228 were taken using a conventional camera.

229

230 *2.3.2 Size-exclusion chromatography for size, molecular weight and branch chain-length*
231 *distribution of starch films*

232 *Molar mass distribution of starch molecules.* The molecular size distributions of starch before
233 and after production of compression-molded films were analyzed using same size-exclusion
234 parameters as described elsewhere (Vilaplana & Gilbert, 2010). Starch films were dissolved
235 in DMSO/LiBr 0.5% (w/w) at a concentration of about 3 mg/ml and heated to 60 °C under
236 stirring overnight. Samples were injected into a Size-exclusion Chromtographer (SECurity
237 1260, Polymer Standard Service, Mainz, Germany) with triple detection (RI, UV and
238 MALLS) and separated using GRAM pre-column, 100Å and 10000Å analytical columns
239 from PSS (Mainz, Germany) at a flow rate of 0.5 ml/min at 60 °C. Calibration was carried out

240 using pullulan standards with molecular weight of 342 to 708000 Da to relate the elution
241 volume V_{el} to the hydrodynamic volume V_h using a dn/dc value of 0.0853 ml/ g and Mark-
242 Houwink parameters $K=2.427*10^{-4}$ dl/ g and $a=0.6804$ (for pullulan standards). The data was
243 processed using WinGPC (PSS, Mainz, Germany) software to get weight distributions of
244 separated starch molecules.

245 *Debranching of starch.* About 50 mg of starch were weighed into a tube and wetted with
246 0.5 ml distilled water and then 4.5 ml DMSO was added and heated in a boiling water bath for
247 1 h and then left stirring overnight to completely dissolution. An aliquot of 0.5 ml was
248 precipitated with 2.5 ml EtOH and centrifuged. The supernatant was discarded before the
249 pellet was dissolved in 4.5 ml water in a boiling water bath for 15 min. To the cool dispersion
250 0.5 ml of 0.1 N acetate buffer, 10 μ l of 100 ppm sodium azide solution and 25 μ l of
251 isoamylase (EC 3.2.1.68, Megazyme, 100 U/ ml). Samples were incubated for 4 h at 37 °C
252 and then starch was precipitated using 25 ml EtOH and centrifuged. The pellet was dissolved
253 in DMSO/LiBr 0.5% (w/w) for 2 h at 80 °C before injection into the SEC system. Since
254 debranched starch molecules are linear chains, the molar mass equals the hydrodynamic
255 volume calculated from the DRI calibration curve from pullulan standards and the degree of
256 polymerization can be calculated by dividing the molar mass by the mass of the
257 anhydroglucose unit (162 Da).

258

259 *2.3.3 Microstructure analysis of film surface and cross-sections using FESEM*

260 Field emission scanning electron microscope (FESEM) images of the cross-section of all
261 starch films were taken using a ZEISS ULTRA 55 model (Zeiss, Germany). The films were
262 previously dehydrated at 0% RH over P_2O_5 and cryo-fractured using liquid nitrogen. The
263 films were placed on graphite stickers and were gold coated. Images were taken using an
264 acceleration voltage of 1.5 kV.

265

266 *2.3.4 Moisture content of starch films*

267 Moisture content of films conditioned at 53% RH was measured gravimetrically after drying
268 at 60 °C for 48 h under vacuum and subsequent equilibration at 0% RH for 2 days at room
269 temperature in sealed chambers containing P₂O₅.

270

271 *2.3.5 Optical properties of starch films: color and internal transmittance*

272 The measurement of the optical properties of starch films equilibrated at 53% RH at 25 °C
273 was carried out using a MINOLTA spectrophotometer (Model CM-3600d, Tokyo, Japan).
274 The reflection spectra (400 to 700 nm, 10 nm bandwidth, specular component included) of the
275 films backed on black and white plates were measured in triplicate at three points of the same
276 film sample. The internal transmittance was measured by applying the Kubelka-Munk theory
277 of the multiple dispersion of reflection spectrum using the reflection spectra of the white and
278 black backgrounds. The CIEL*a*b* color coordinates (illuminant D65 and observer 10°)
279 were obtained from the reflectance of an infinitely thick layer of the material according to
280 Hutchings (1999).

281

282 *2.3.6 Tensile properties*

283 Tensile properties were determined in 8 replicates using a Universal testing machine (Stable
284 Micro System TA, XT plus, Haslemere, England) following the ASTM standard method
285 (D882.ASTM D882, 2001). The conditioned films (25 °C, 53% RH) were cut into
286 25 mm x 80 mm pieces and mounted into the equipment with a stretching of 50 mm/ min⁻¹.
287 Stress at break, maximum elongation and Young's modulus were calculated from the stress-
288 strain curves, based on the average film thickness measured at 6 points.

289

290 *2.3.7 Barrier properties*

291 Water vapor permeability (WVP) was determined gravimetrically at 25 °C using a
292 modification of the ASTM E96-95 gravimetric method (1995) for hydrophilic films. Starch
293 film samples were cut into circles of ø3.5 cm and mounted into Payne permeability cups
294 (Elcometer SPRL, Hermelle/s Argenteau, Belgium) that were filled with 5 ml of distilled
295 water (100% RH). The cups were placed into pre-equilibrated cabinets containing saturated
296 solutions of magnesium nitrate (53% RH) with a fan on the top of the cup. The cups were
297 weighed periodically (1.5 h to 24 h) using an analytical balance with ±0.00001 g accuracy.
298 The slope of the weight loss versus time was plotted and the water vapor transmission rate
299 (WVTR) and WVP were calculated using duplicates.

300 Oxygen permeability of starch films equilibrated at 53% RH was measured using Ox-Tran
301 equipment (MOCON Model 1/50, Minneapolis, USA). Starch films of 50 cm² were placed
302 into the equipment at 25 °C and 53% RH. Oxygen permeability was calculated by multiplying
303 oxygen transmission rate and the average film thickness of the starch film determined at five
304 points. The measurement was done in duplicate.

305

306 *2.3.8 Thermal analysis of starch films*

307 Thermal properties of the starch films were measured using differential scanning calorimetry
308 (DSC 1 StareSystem, Mettler-Toledo, Inc., Switzerland) and thermogravimetric analyzer
309 (TGA/SDTA 851e, Mettler Toledo, Schwarzenbach, Switzerland). Samples were conditioned
310 for 1 week at 0% RH before analysis. DSC curves were obtained by heating the sample from
311 25 °C to 160 °C at 5 °C/ min and holding for 5 min at 160 °C. Samples were then cooled to
312 10 °C and rested for 5 min and a second heating cycle was performed to 160 °C at 10 °C/ min.
313 TGA analysis was performed by heating the samples from 25 °C to 600 °C at a heating rate of
314 10 °C/min. Thermal analysis were performed under a nitrogen flow (10 mL/min). Both
315 measurements were performed in triplicates.

316

317 *2.3.9 In-vitro antioxidant activity of films using DPPH* assay*

318 About 1g of film was weighed into a 100 ml bottle and 50.0 ml distilled water was added. The
319 film was suspended in the water using a roto-stator for about 1 min and afterwards stirred
320 about 12 h at 200 rpm at room temperature. An aliquot of the starch dispersion was filtered
321 using a 0.45 µm filter and used for the DPPH assay as described in the 2.2.3 section. The
322 measurement was carried out in triplicates.

323

324 *2.4 Statistical analysis*

325 IBM SPSS Statistics 25.0.0 software has been used for analysis of variance (ANOVA) and
326 Tukey's HSD post hoc test in case of equal replicates and Gabriel post hoc test for unequal
327 amount of replicates. In case of duplicates a simple t-test has been used for comparison.

328 3. RESULTS AND DISCUSSION

329 3.1 Extraction and characterization of phenolic compounds from sunflower hulls

330 The milling process was initially studied to optimize the yield for extraction of phenolic
331 compounds using different milling fractions (schematic Fig. 1, milled raw material, material
332 <0.6mm and <0.2mm). The material has been shown to be very tough during milling,
333 requiring long time and several repetitions. In general, smaller particle sizes resulted in higher
334 extraction yields of phenolic compounds measured as total phenolic content. The highest
335 values of 498 mg GAE/100 g dry milled sunflower hulls were achieved using material
336 <0.2 mm, which represents 20% of the material from the first milling fraction. However, from
337 a time-efficient and economical point of view, around 90% of the raw material could be
338 milled to <0.6 mm within two milling stages, which was used for all further analysis (red
339 marked in Fig. 1).

340 In a second step the extraction conditions have been optimized using different solvent and
341 time and were evaluated in terms of total phenolic acid content (Table 1). Methanol extracts
342 showed better yields in terms of total phenolic content and this solvent was selected to obtain
343 the active extracts used for preparing active starch films. Likewise, the final phenolic extract
344 were obtained with 80% aqueous MeOH at a hull:solvent ratio 1:10 under constant stirring for
345 30 min at room temperature in order to reduce the solvent use. Longer times (1h, Table 1) and
346 repetitive extraction up to three times (3x extraction, Table 1) did not improve yields
347 significantly and is not economically viable, due to the great amount of extraction solvent
348 used. Several studies reported similar results between 190 up to 400 mg GAE/100 g dry
349 sunflower hulls using Folin reagent (De Leonardis et al., 2005; Taha, Wagdy, Hassanein, &
350 Hamed, 2012).

351 **Table 1.** Total phenolic content in mg GAE/100 g DM hulls using different extraction
352 solvent, times, repeated extractions, material particle size and hull:solvent ratio.

Extraction	80% MeOH	80% EtOH
30min, 1x extraction, entire sample , 1:20 ratio	146 ± 10	134 ± 10
1h , 1x extraction, <0.6mm, 1:20 ratio	157 ± 12	145 ± 10

30min, 3x extraction , <0.6mm, 1:20 ratio	194 ± 9.0	176 ± 7.0
30min, 1x extraction+ washing filter , <0.6mm , 1:20 ratio	277 ± 20	176 ± 17
30min, 1x extraction+ washing filter, <0.6mm , 1:10 ratio	137 ± 20	

353
354 The three main phenolic acids identified and quantified using HPLC-DAD are summarized in
355 Table 2 for the 30 min extraction at room temperature using 80% aqueous MeOH extract and
356 80% aqueous EtOH extract at a 1:10 solids:solvent ratio. In total 11 peaks were detected
357 (supplementary Table S1): three peaks were assigned to be isomers of caffeoylquinic acid and
358 one was expected to be a dicaffeoylquinic acid derivate (Chromatographic profile and
359 chemical structure in supplementary Figure S1) and some peaks were unknown. The
360 assignment of phenolic acids was in accordance with Weisz, Kammerer, and Carle (2009)
361 using equivalent HPLC conditions.

362 **Table 2.** HPLC results of individual phenolic acid content at 325 nm and EC₅₀ values from
363 DPPH* assay of aqueous MeOH and EtOH sunflower hull extracts from <0.6 mm material,
364 extracted 30 min at room temperature at 1:10 hull:solvent ratio and washed filter.

Extraction	Phenolic acid [mg/100g hulls]			EC ₅₀ values [mg/mg DPPH*]	
	Chlorogenic acid	Caffeic acid	Dicaffeoyl-quinic acid	<0.6mm material	Freeze-dried extract
80% aqueous MeOH	78.3± 16.2	1.4 ± 0.26	2.6 ± 0.57	73.5	4.41*
80% aqueous EtOH	57.3± 1.22	1.0 ± 0.02	3.3 ± 0.02	88.7	4.43*

365 * freeze-dried extract for 80% aqueous MeOH was 6wt% of the dry raw material, 5wt% for 80% aqueous EtOH
366 Extraction with 80% aqueous MeOH resulted in the highest content of the three identified
367 phenolic acids with 82.3 mg/ 100 g dry sunflower hulls. Differences between determinations
368 using Folin reagent and HPLC-DAD are explained since Folin determination is sensitive to
369 other reducing non-phenolic components such as sugars and amino acids that interfere with
370 that analysis (Georgé, Brat, Alter, & Amiot, 2005). Chlorogenic acid was identified as the
371 main phenolic compound with 95% and 93% in methanolic and ethanolic extracts,
372 respectively, showing that the extraction of different phenolic acids depends on the extraction
373 solvent. Weisz et al. (2009) and Szydłowska-Czerniak et al. (2011) reported similar amounts
374 (40-86 mg total phenols/ 100 g dry hulls) of the total phenolic compounds of different
375 sunflower hulls, with chlorogenic acid as main component and minor amounts of coumaric
376 and ferulic acid derivates, mono-caffeoylquinic and dicaffeoylquinic acid derivates.

377 The antioxidant capacity of the phenolic extracts were determined using DPPH* assay and
378 EC₅₀ values were calculated based on mg of dry sunflower hulls/ mg DPPH* (Table 2). It was
379 shown that 73.5 mg hulls are necessary to reduce 50% of 1 mg of DPPH* when extracted
380 with 80% aqueous MeOH. In comparison, total phenolic content by Folin reagent
381 determination showed 137 mg GAE/100g dry sunflower hulls, which represents 0.14% of the
382 material. Accounting for 0.14% of the starting material being phenolic compounds, the EC₅₀
383 value was 0.102 mg of GAE/mg DPPH*, which is higher than the EC₅₀ value of pure gallic
384 acid (0.034 mg/ mg DPPH*) but close to the EC₅₀ value of caffeic and chlorogenic acids
385 (0.083 and 0.151 mg/ mg DPPH*). Since the methanolic extract was evaporated and freeze-
386 dried before addition to starch films, EC₅₀ value were calculated based on the dry extract yield
387 of 6wt%, resulting in EC₅₀ values of 4.41 mg dry extract/ mg DPPH* (Table 2).

388

389 Antibacterial activity against *E.coli* and *Listeria innocua* was determined. However, no clear
390 MIC was detected at concentrations as high as 100 mg extract/ ml (supplementary Figure S2),
391 which was in contrast with previously reported data. Taha et al. (2012) studied the
392 antimicrobial activity of sunflower hull extract against five food borne pathogenic bacteria (*E.*
393 *coli*, *Listeria monocytogenes*, *Bacillus cereus*, *Staphylococcus aureus*, *Salmonella*
394 *typhimurium*) at a concentration of 5 mg extract/ ml using disc diffusion method and showing
395 inhibition of growth of *E.coli* of a similar 80% aqueous MeOH extract. It is important to point
396 out that in this study, there was a clear change in cell growth at around 40 mg/ml for *Listeria*
397 *innocua* and *E.coli*, represented by a spot coloration rather than full coloration of the wells
398 (supplementary Figure S2). That might me be due to a bacteriostatic action of the extract
399 where cell growth inhibition occurred but no cell death. Further *in vitro* and *in vivo* analysis
400 on different food products should be carried out to confirm the bacteriostatic or bactericidal
401 action of the extract and its potential as anti-bacterial agent in food packaging applications.

402 3.2 Preparation and evaluation of starch films with antioxidant extract

403 3.2.1 Changes in molecular structure of starch determined as molecular weight distributions
 404 and branch chain-length distribution using size-exclusion chromatography

405 The changes in molecular structure of starch caused by thermal processing were monitored for
 406 the starch films in comparison with native starch, in terms of the molar mass distribution of
 407 the starch macromolecules and the branch chain-length distribution after debranching with
 408 isoamylase (Fig. 3, Table 3). The starting native potato starch exhibited a bimodal size
 409 distribution (Fig. 3a) corresponding to the distinct amylopectin ($R_h \sim 20\text{-}100$ nm) and amylose
 410 ($R_h \sim 1 - 20$ nm) population, with a weight-average molecular weight \overline{M}_w of 9.1×10^6 Da
 411 (Table 3).

412 **Table 3.** Sample abbreviation and composition of starch-glycerol films with and without
 413 antioxidant extract (AOE). Number-average molecular weight \overline{M}_n , weight-average molecular
 414 weight \overline{M}_w and polydispersity D for branched starches using light scattering and peak
 415 maximum of degree of polymerization X_{DP} in the three regions of debranched samples and
 416 height ratio of AP2/API (AP-amylopectin, AM-amylose) using the DRI calibration.

Sample Abbreviation	Composition [g]			Branched Starch			Debranched Starch			
	starch	Gly	AOE	\overline{M}_w [MDa]	\overline{M}_n [MDa]	D	$X_{DP,AP1}$	$X_{DP,AP2}$	AP2/API	$X_{DP,AM}$
Native starch				9.10	8.07	1.13	26	48	0.93	7475
CS_7G	40	7	-	1.03	0.61	1.70	24	46	1.06	464
CS_10G	40	10	-	3.57	2.36	1.36	24	50	1.08	1240
SS_9.5G_0.5A	40	9.5	0.5	1.67	1.34	1.24	25	49	1.00	996
SS_9G_1A	40	9	1	2.45	1.81	1.35	27	49	0.94	920
SS_8G_2A	40	8	2	1.88	1.18	1.59	24	49	1.05	693
SS_7G_3A	40	7	3	1.29	0.69	1.85	28	49	0.96	497

417

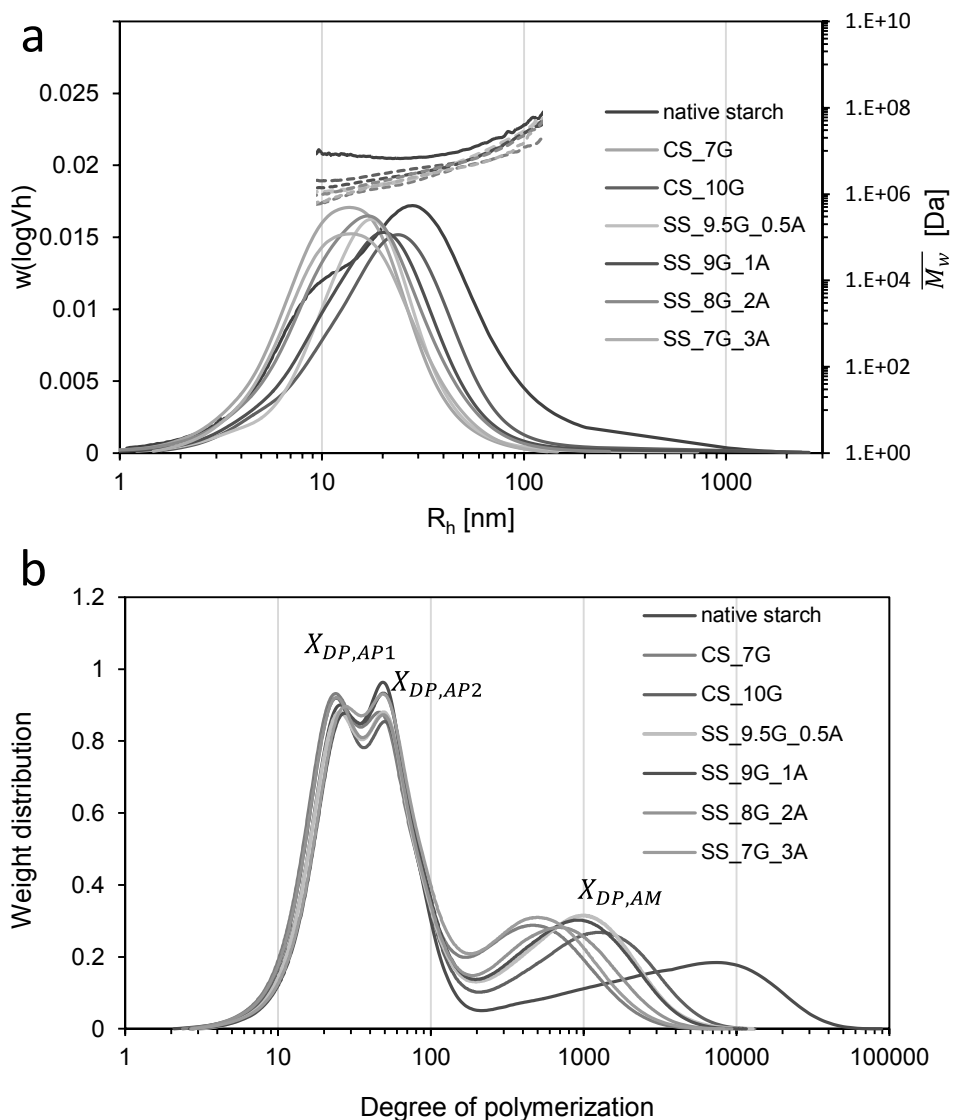
418 The thermal processing of the starch films resulted in a monomodal size distribution together
 419 with a shift of the size distribution to smaller sizes where no distinct contributions of the
 420 amylopectin and amylose molecules were further detected. This was correlated with a
 421 noticeable decrease in the weight-average molar mass \overline{M}_w (R_h) obtained from the MALLS
 422 detector for all processed samples, associated with the degradation processes induced during

423 the thermal-shear processing (Table 3). In addition, the reduction in the amounts of glycerol
424 (CS_10G to CS_7G) resulted in a further decrease of the molar mass and size distribution of
425 starch films; starch films with added AOE showed the same trend. It is well known that starch
426 is susceptible to shear-induced and thermal breakdown while an increasing amount of
427 glycerol protected against starch degradation during processing of films (Carvalho, Zambon,
428 Curvelo, & Gandini, 2003). In addition, Liu, Halley, and Gilbert (2010) reported a similar
429 trend of starch chain scission and shift towards monomodal weight distribution of starch after
430 extrusion attributed to amylopectin being highly susceptible to shear degradation.

431 In order to further study the effect of thermal-mechanical degradation during processing on
432 the amylopectin and amylose populations, the branch chain-length distribution for the intact
433 starch and the films were evaluated after enzymatic debranching. The branch chain-length
434 distribution of starch showed two distinctive peaks (Fig. 3b): one bimodal amylopectin peak
435 <100 DP ($X_{DP,AP}$) and one amylose peak >100 DP ($X_{DP,AM}$). The peak maxima are
436 summarized in Table 3. The bimodal distribution of the amylopectin peak is associated to the
437 amylopectin branching pattern into defined clusters with single-lamellar branches (AP1 with
438 $X_{DP,AP1} \sim 5$ to 35) and lamella-spanning branches (AP2 with $X_{DP,AP2} \sim 35$ to 100) (Vilaplana &
439 Gilbert, 2010; Vilaplana, Meng, Hasjim, & Gilbert, 2014; Wang & Wang, 2001).

440 A clear shift in the peak of the long-chain amylose fraction was observed for all starch films
441 compared to the native starch ($X_{DP,AM}$ in Fig. 3b and Table 3), thus indicating that also the
442 long-branch fractions were sensitive to hydrolytic cleavage during processing. Wang and
443 Wang (2001) reported similar patterns in acid thinned potato starch with a decrease of long-
444 chain molecules of amylose in debranched starches and a shift of the amylose fraction to
445 lower chain-length. The relatively constant peak height ratio (AP2/AP1 in Table 3) showed
446 that the branching pattern of debranched amylopectin was not significantly altered indicating
447 that molecules were randomly broken. The same trend was reported by Liu et al. (2010) who
448 investigated the effect of extrusion on starch degradation. These authors reported that

449 debranched samples showed no significant change in the shape of the branch chain-length
 450 distribution after extrusion and attributed this to a non-selective breaking of glycosidic bonds
 451 within the branches. It can be assumed that mainly branching points were cleaved which
 452 would preserve the distribution of individual branch lengths. There was only a slight increase
 453 in AP2/AP1 height ratio of starch films compared to the native starch which indicated that the
 454 short branches (AP1) were more sensitive to thermal degradation than the longer branches in
 455 the amylopectin population AP2.



456
 457 **Figure 3.** a) SEC weight distribution and weight-average molecular weight \overline{M}_w as function
 458 of hydrodynamic radius R_h for native potato starch and starch films dissolved in DMSO/LiBr
 459 0.5% and b) SEC weight distribution of debranched starches as function of their degree of
 460 polymerization (DP).

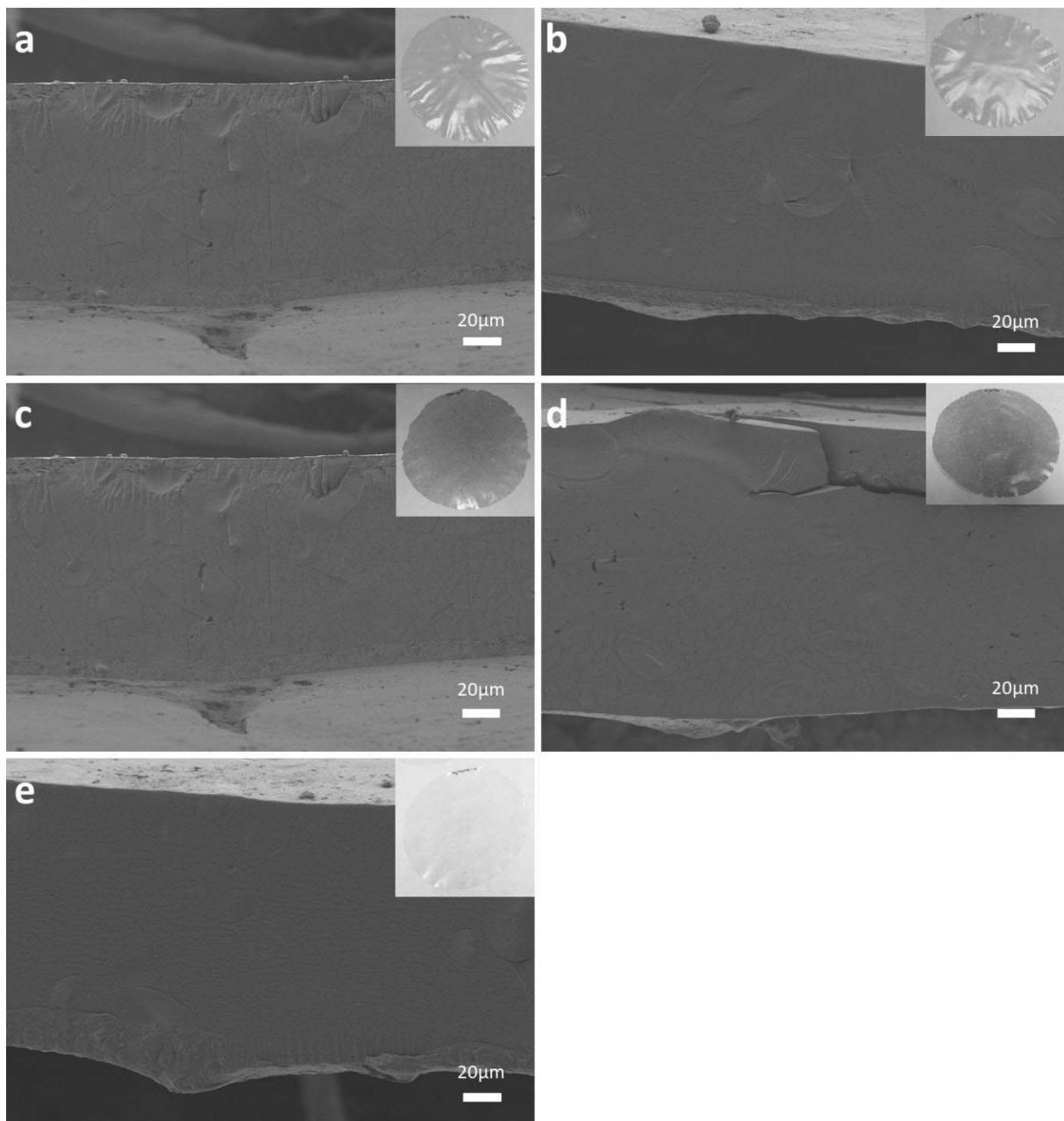
461

462 In summary, our study demonstrated that both amylose and amylopectin fractions were
463 affected by the thermo-mechanical degradation, as evidenced by the decrease in the weight-
464 average molecular weight \overline{M}_w and size distribution of the starch macromolecules and the
465 evident changes in the long-chain amylose fraction of debranched samples.

466

467 *3.2.2 Starch film microstructure*

468 The resulting starch films produced by compression molding had a thickness between 181 μm
469 and 216 μm . Images of the film cross-sections using FESEM are shown in Fig. 2. The films
470 showed smooth surfaces and no cracks, no pores or phase separations. The phenolic extract
471 was successfully integrated into the starch-glycerol matrix.



472
 473 **Figure 2.** FESEM images of cross sections of starch films with a) 0.5g antioxidant extract
 474 (AOE) (SS_9.5G_0.5A), b) with 1g AOE (SS_9G_1A), c) with 2 g AOE (SS_8G_2A), d)
 475 with 3 g AOE (SS_7G_3A) and e) without AOE (CS_7G) . Digital images of films are
 476 displayed in the upper right corner.

477

478 3.2.3 Optical properties of the films

479 The optical properties of the films were measured to evaluate their color and transparency
 480 (Hutchings, 1999). The internal transmittance (T_i) spectra are shown in the supplementary
 481 (supplementary Figure S3). High values of T_i correspond to films with great homogeneity and
 482 hence transparency, whereas low values of T_i are typical for more opaque or colored films.

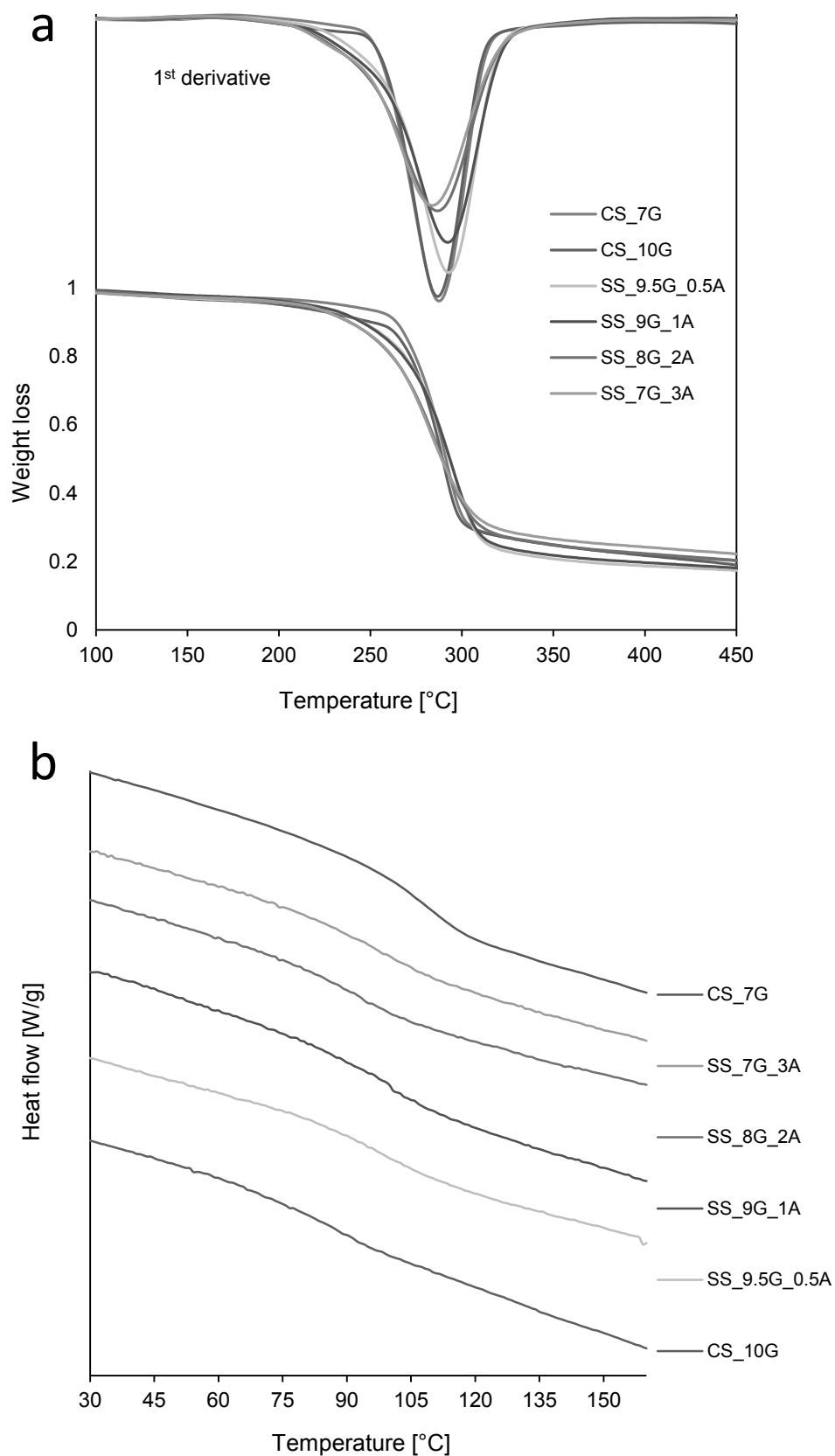
483 The control starch film exhibited high values of T_i at entire wavelength range which reflected
484 the high level of film transparency. Films containing AOE showed a decrease in T_i at low
485 wavelength associated with the selective absorption of the AOE compounds. The higher the
486 AOE concentration, the lower the T_i values and more colored films.

487 Color parameters L^* , a^* , b^* (supplementary Table S1) revealed the effect of AOE on the film
488 color. The films appeared more yellowish-brownish with increasing amount of AOE.
489 Lightness L^* was highest for the control films plasticized with glycerol and an increase in the
490 AOE amount decreased lightness. The color coordinate a^* increased with the content of AOE
491 while parameter b^* slightly decreases representing a change towards more reddish color as the
492 AOE concentration rose.

493 Although transparency of packaging material is a valuable parameter, color formation in the
494 films can be of advantage as consumer perception might be attracted to these kinds of colors
495 in packaging, especially for products such as chocolate or nuts, at the same time that the films
496 could better protect the products against negative effects of light.

497 *3.2.4 Thermal behavior of the films*

498 Thermal gravimetric analysis was used to determine the thermal decomposition and stability
499 of the dry starch films. The results of the TGA curves and their first derivative are shown in
500 Fig. 4a (numerical data in Table 4). The small mass loss below 100 °C can be mainly ascribed
501 to unbounded water loss. The following mass loss till the onset temperature of the thermal
502 decomposition at around 250 °C can be related to the evaporation/ decomposition of both the
503 glycerol and bonded water in starch films. Starch thermal decomposition occurred between
504 250 °C and 300 °C, without remarkable differences between samples, although starch films
505 with high amount of AOE showed a slight shift towards lower degradation temperature
506 (Fig. 4a). However, starch films with AOE had a lower weight loss up to 300 °C, thus
507 suggesting the presence of little amounts of ash content in the extracts.



508
 509 **Figure 4.** a) TGA curves and first derivative of starch films with and without AOE and b)
 510 DSC curves of all starch films.
 511

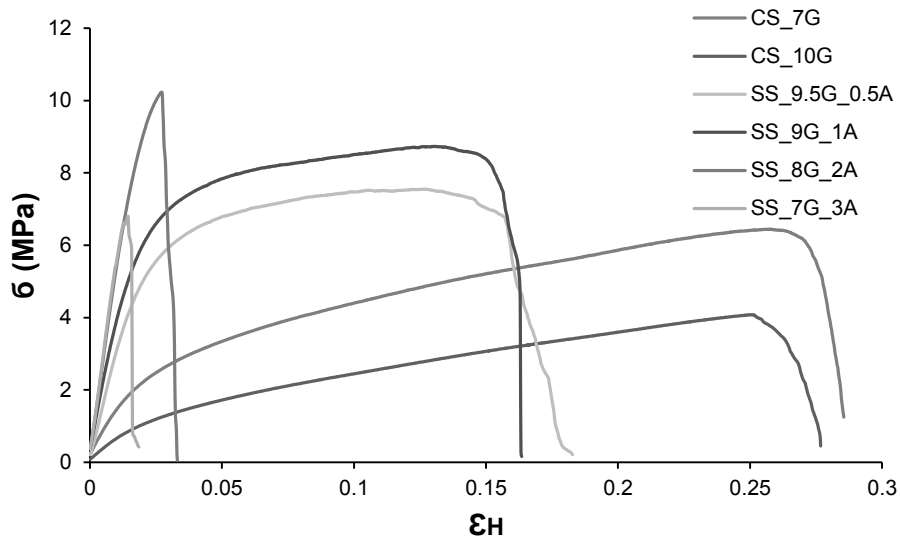
512 The glass transition temperature T_g is an important parameter at determining the mechanical
513 properties of amorphous polymers (Biliaderis, Page, Maurice, & Juliano, 1986). Often, it is
514 desirable to decrease T_g just below ambient temperature and obtain supple and deformable
515 rubbery materials. The T_g of completely dried films were determined using DSC for the
516 purposes of analyzing the potential plasticizing effect of the AOE. The onset and midpoint are
517 shown in Table 4 (curves in Fig. 4b). For the AOE-free samples the increase in the glycerol
518 content provoked the expected decrease in the T_g (Chang, Abd Karim, & Seow, 2006;
519 Forssell, Mikkilä, Moates, & Parker, 1997). However, the different degrees of partial
520 substitution of glycerol by AOE in the films did not provoke significant changes in the T_g
521 values. In fact, control films without AOE with the minimum amount of glycerol (CS_7G)
522 exhibited closer T_g values to that AOE containing films than control film with the maximum
523 glycerol content. Likewise, this transition was more extended in films with AOE. This
524 suggests that the interaction of AOE compounds with the starch chains induced restrictions in
525 the molecular mobility in the amorphous phase, interfering the glycerol plasticizing effect.
526 Nevertheless, the greater level of starch de-polymerization when the glycerol content
527 decreased would also contribute to the T_g values in the different matrices.

528

529 *3.2.5 Tensile properties*

530 Tensile properties of all films were measured and the obtained stress-strain curves (Fig. 5)
531 were used to determine Young's modulus and tensile strength and elongation at break (Table
532 4). Starch films without or with low amounts of AOE showed a typical elastic behavior in the
533 initial region where the low Young's modulus was determined and when the yield point was
534 reached plastic flow started until the film ruptured. The elongation at break for glycerol-starch
535 films without AOE was 26.0% and 25.3% with stress at break of 4.31 MPa and 5.36 MPa, for
536 the highest and lowest amount of glycerol, respectively. Glycerol is a well-known plasticizer

537 that increases the mobility of the polymer chains and makes the films more flexible/extensible
538 (Myllärinen, Partanen, Seppälä, & Forssell, 2002).



539

540 **Figure 5.** Stress-strain curve of starch films with glycerol and different amounts of phenolic
541 extract.

542 The glycerol substitution by AOE at the two lowest levels showed similar behavior as AOE-
543 free films, but exhibited a twofold and fivefold increase in tensile strength. This could be
544 attributed to the hydrogen bond interactions between starch chains and the AOE phenolic
545 acids, contributing to the film cohesiveness and low flexibility. These kind of interactions
546 were intensified in the films containing the highest levels of glycerol substitution, resulting in
547 changes in their tensile behavior. The stress-strain curves of these films showed a linear
548 region until a higher strain, with a fivefold to tenfold higher Young's modulus, which
549 indicated greater film rigidity. However, these films exhibited low values of elongation at
550 break (1.23% and 4.23%, respectively) being less flexible and more brittle.

551 As concerns tensile behavior, although almost constant T_g values were obtained for the dry
552 matrices with different degree of glycerol substitution, their differences in the film water
553 affinity could also affect the mechanical response. The equilibrium moisture content of the
554 films (Table 4) became lower when the glycerol content decreased. This lower amount of
555 water content could also contribute to the increase in the film Young's modulus when the

556 AOE content rose, since water has a strong plasticizing effect. In addition, the different degree
557 of starch degradation (see molecular weight results above) in the different films could affect
558 their mechanical properties but this effect could be overlapped with the plasticizing effect of
559 glycerol or the effect of added phenolic extract.

560

561

Table 4. Physical properties of starch films with phenolic extract.

Starch [g]	Thickness*		Moisture* %	TGA peak [°C]	T _g		EC ₅₀ [mg film/mg DPPH]	OP 10 ¹⁴ (cm ³ /ms Pa)	WVP gmm/kPahm ²	Tensile properties		
	[μm]				Onset [°C]	Midpoint [°C]				Elongation [%]	Tensile strength [MPa]	Young's modulus
CS_7G	0.216 ^c		7.17±0.03 ^a	285±0.5 ^{b,c}	100±2 ^b	117±10 ^b	n.d	1.63±0.26	7.62±0.88	25.3±3.94 ^c	5.36±0.93 ^a	79±20 ^a
CS_10G	0.188 ^b		12.7±0.12 ^d	284±0.5 ^b	54±8 ^a	70±7 ^a	n.d	6.37±0.65	11.5±0.14	26.0±5.95 ^c	4.73±1.11 ^a	55±20 ^a
SS_9.5G_0.5A	0.198 ^a		9.28±0.02 ^c	287±0.5 ^c	100±10 ^b	105±3 ^b	318±0.8 ^d	8.05±0.12	15.1±0.40	14.8±2.80 ^b	7.90±0.84 ^c	245±26 ^b
SS_9G_1A	0.198 ^{a,b}		8.67±0.09 ^b	286±0.5 ^{b,c}	83±10 ^{a,b}	98±8 ^b	211±0.8 ^c	6.80±0.11	12.2±0.78	13.8±4.32 ^b	7.43±0.70 ^{b,c}	223±46 ^b
SS_8G_2A	0.181 ^{a,b}		8.28±0.12 ^b	281±0.9 ^a	81±8 ^b	92±9 ^{a,b}	122±9.6 ^b	4.36±0.33	9.95±1.90	4.23±3.82 ^a	8.24±1.54 ^c	441±134 ^c
SS_7G_3A	0.182 ^b		7.57±0.40 ^a	281±1.4 ^a	94±15 ^b	105±13 ^b	71.3±3.1 ^a	3.20±0.30	8.22±0.22	1.23±0.68 ^a	5.56±1.68 ^{a,b}	580±107 ^d

562 *thickness – average of 48 replicates and Tukey's HSD post hoc test, moisture content – average of 3 replicates and Tukey's HSD post hoc test, TGA DPPH – average of 3 replicates
563 and Tukey's HSD post hoc test, OP and WVP – average of 6-8 replicates, tensile testing – average of 6-8 replicates using Gabriel post hoc test, T_g – average of duplicates and t-test
564 (p<0.05)

565

566 *3.2.6 Barrier properties*

567 Oxygen permeability (OP) values are shown in Table 4. Control films showed the
568 susceptibility of starch as barrier to the glycerol content as lower content of glycerol
569 decreased OP values. Similar effects of glycerol content has been shown previously on
570 compression molded films of starch (Arvanitoyannis, Psomiadou, & Nakayama, 1996). The
571 glycerol substitution by the phenolic extract into the films slightly increased OP values at the
572 lowest substitution level, however, the oxygen barrier capacity increased as the phenolic
573 extract concentration rose. This improvement of the oxygen barrier capacity could linked to
574 the decrease of glycerol content in the film and hence the formation of a more tightly packed
575 network structure with reduced molecular mobility (Arvanitoyannis et al., 1996).

576 Water vapor permeability was measured at 25 °C and at a 53-100% RH gradient. As occurred
577 with the OP values. Films with the lowest substitution of glycerol by the phenolic extract
578 (SS_9.5G_0.5A) resulted in a slight increase of WVP values, but a subsequent decreased
579 occurred when concentration of phenolic extract rose. The lower WVP values could be
580 explained by the lower amount of glycerol in the films as seen for the control films but also to
581 the interactions between the compounds of the antioxidant extract and starch which might lead
582 to a lower affinity of the starch films with water molecules, as reveals the decrease of the
583 equilibrium moisture content. That is in accordance with previous results where water vapor
584 transfer rate has been shown to be proportional to total plasticizer content (polyols and water)
585 within the polymer matrix (Arvanitoyannis et al., 1996).

586

587 *3.2.7 Determination of antiradical activity using DPPH* bleaching method*

588 An increased addition of the phenolic extract to the starch film resulted in lower EC₅₀ values
589 which in turn proved higher antiradical activity of these films (Table 4). Based on the added
590 amount of phenolic extract (1, 2, 4 and 6% based on starch-glycerol formulation) multiplied
591 with the EC₅₀ values from the prepared films offers an estimation of extract needed to reduce

592 50% of one mg DPPH*: 3.18 mg, 4.22 mg 4.88 mg and 4.26 mg which is accordance with the
593 EC₅₀ value of the methanolic extract reported above of 4.41 mg extract/ mg DPPH* (Table 2).
594 Hence, no antiradical activity of the phenolic extract was lost during the film preparation.
595 Similar amounts were reported by Pastor, Sánchez-González, Chiralt, Cháfer, and González-
596 Martínez (2013) incorporating resveratrol as antioxidant into chitosan and methylcellulose
597 films and reported EC₅₀ values of about 50 mg film/ mg DPPH* using 5% of antioxidant in
598 the films which is in the same range as the films produced in this study with 6% as the highest
599 amount of phenolic extract added (SS_7G_3A) and an EC₅₀ value of 71 mg films/mg DPPH*.
600 Nevertheless, in this study the films were dispersed into water and DPPH* activity of the
601 water solution was measured. The antioxidant effect will have to be further evaluated in food
602 contact applications monitoring changes during storage and release of the phenolic
603 compounds into the product since the activity of the antioxidant extract in the films would
604 become more relevant in wet systems and direct contact with a food product (Bonilla, Atarés,
605 Vargas, & Chiralt, 2012).

606

607 **CONCLUSIONS**

608 This study shows the potential use of utilizing sunflower hulls as a valuable source of a
609 natural antioxidant extract. The extraction was shown to be fast and easy using 80% aqueous
610 MeOH. Chlorogenic acid was identified as the main active compound with expected
611 antiradical activity against DPPH*. Different amounts of the phenolic extract, 1-6 wt% based
612 on the starch-glycerol formulation for films, were successfully incorporated into compression-
613 molded films preserving their antiradical activity against DPPH*. The incorporation of up to
614 6% active compound generated less stretchable and stiffer films. The change in tensile
615 properties was mainly attributed to the interactions of the phenolic compounds with the starch
616 polymer. All films showed good oxygen and water vapor barrier properties and the main
617 changes in barrier properties can be attributed to the reduction of glycerol as it was partially

618 replaced by the phenolic extract from sunflower hulls, and the associated difference in the
619 equilibrium water content in the films. The films developed an increased yellow-brownish
620 color with higher amount of extract but kept their transparency. The heat-shear treatment
621 during melt blending and compression molding process induced a reduction in the molecular
622 weight of starch affecting both the amylose and amylopectin populations. However, higher
623 amounts of glycerol slightly prevented starch degradation. The starch films showed good
624 thermal stability until 250 °C and a glass transition at 80 – 100 °C depending on the glycerol
625 content, whereas the incorporation of the phenolic extract showed little influence on the
626 thermal behavior of the films.

627 The study demonstrates the potential use of agricultural by-products to be re-utilized as raw
628 material to produce 100% renewable and recyclable active food packaging material or
629 coatings by compression-molding. The application of the developed active starch films with
630 phenolic extracts from sunflower hulls in direct contact with foodstuff will be further
631 examined.

632

633 **ACKNOWLEDGEMENTS**

634 This work was supported by the Swedish Research Council Formas [942-2015-550] and by
635 the project AGL2016-76699-R from Spanish Ministerio de Educación y Ciencia. The authors
636 would like to acknowledge Grefusa (Alzira, Spain) for the donated sunflower hull waste.

637

638 **REFERENCES**

- 639 Arvanitoyannis, I., Psomiadou, E., & Nakayama, A. (1996). Edible films made from sodium caseinate,
640 starches, sugars or glycerol. Part 1. *Carbohydrate Polymers*, 31(4), 179-192.
- 641 Biliaderis, C. G., Page, C. M., Maurice, T. J., & Juliano, B. O. (1986). Thermal characterization of rice
642 starches: A polymeric approach to phase transitions of granular starch. *Journal of agricultural
643 and food chemistry*, 34(1), 6-14.
- 644 Bonilla, J., Atarés, L., Vargas, M., & Chiralt, A. (2012). Edible films and coatings to prevent the
645 detrimental effect of oxygen on food quality: Possibilities and limitations. *Journal of food
646 Engineering*, 110(2), 208-213.

- 647 Bonilla, J., Talón, E., Atarés, L., Vargas, M., & Chiralt, A. (2013). Effect of the incorporation of
648 antioxidants on physicochemical and antioxidant properties of wheat starch–chitosan films.
649 *Journal of food Engineering*, 118(3), 271-278.
- 650 Brand-Williams, W., Cuvelier, M. E., & Berset, C. (1995). Use of a free radical method to evaluate
651 antioxidant activity. *LWT - Food Science and Technology*, 28(1), 25-30.
- 652 Cancalon, P. (1971). Chemical composition of sunflower seed hulls. *Journal of the American Oil
653 Chemists' Society*, 48(10), 629.
- 654 Carvalho, A. J. F., Zambon, M. D., Curvelo, A. A. S., & Gandini, A. (2003). Size exclusion
655 chromatography characterization of thermoplastic starch composites 1. Influence of
656 plasticizer and fibre content. *Polymer Degradation and Stability*, 79(1), 133-138.
- 657 Chang, Y. P., Abd Karim, A., & Seow, C. C. (2006). Interactive plasticizing–antiplasticizing effects of
658 water and glycerol on the tensile properties of tapioca starch films. *Food Hydrocolloids*, 20(1),
659 1-8.
- 660 Dainelli, D., Gontard, N., Spyropoulos, D., Zondervan-van den Beuken, E., & Tobback, P. (2008). Active
661 and intelligent food packaging: legal aspects and safety concerns. *Trends in Food Science &
662 Technology*, 19, S103-S112.
- 663 De Leonardis, A., Macciola, V., & Di Domenico, N. (2005). A first pilot study to produce a food
664 antioxidant from sunflower seed shells (*Helianthus annuus*). *European Journal of Lipid
665 Science and Technology*, 107(4), 220-227.
- 666 Forssell, P. M., Mikkilä, J. M., Moates, G. K., & Parker, R. (1997). Phase and glass transition behaviour
667 of concentrated barley starch-glycerol-water mixtures, a model for thermoplastic starch.
668 *Carbohydrate Polymers*, 34(4), 275-282.
- 669 Fox, G. J. (2000). Natural red sunflower anthocyanin colorant with naturally stabilized color qualities,
670 and the process of making. Google Patents.
- 671 Georgé, S., Brat, P., Alter, P., & Amiot, M. J. (2005). Rapid Determination of Polyphenols and Vitamin
672 C in Plant-Derived Products. *Journal of agricultural and food chemistry*, 53(5), 1370-1373.
- 673 Ghasemlou, M., Aliheidari, N., Fahmi, R., Shojaee-Aliabadi, S., Keshavarz, B., Cran, M. J., & Khaksar, R.
674 (2013). Physical, mechanical and barrier properties of corn starch films incorporated with
675 plant essential oils. *Carbohydrate Polymers*, 98(1), 1117-1126.
- 676 Houdkova, M., Rondevaldova, J., Doskocil, I., & Kokoska, L. (2017). Evaluation of antibacterial
677 potential and toxicity of plant volatile compounds using new broth microdilution
678 volatilization method and modified MTT assay. *Fitoterapia*, 118, 56-62.
- 679 Hutchings, J. B. (1999). *Instrumental specification*. In *Food colour and appearance* (pp. 199-237):
680 Springer
- 681 Jiménez, A., Fabra, M. J., Talens, P., & Chiralt, A. (2012). Edible and biodegradable starch films: a
682 review. *Food and Bioprocess Technology*, 5(6), 2058-2076.
- 683 Liu, W.-C., Halley, P. J., & Gilbert, R. G. (2010). Mechanism of Degradation of Starch, a Highly
684 Branched Polymer, during Extrusion. *Macromolecules*, 43(6), 2855-2864.
- 685 Myllärinen, P., Partanen, R., Seppälä, J., & Forssell, P. (2002). Effect of glycerol on behaviour of
686 amylose and amylopectin films. *Carbohydrate Polymers*, 50(4), 355-361.
- 687 Oriani, V. B., Molina, G., Chiumarelli, M., Pastore, G. M., & Hubinger, M. D. (2014). Properties of
688 cassava starch-based edible coating containing essential oils. *Journal of food science*, 79(2),
689 E189-E194.
- 690 Pastor, C., Sánchez-González, L., Chiralt, A., Cháfer, M., & González-Martínez, C. (2013). Physical and
691 antioxidant properties of chitosan and methylcellulose based films containing resveratrol.
692 *Food Hydrocolloids*, 30(1), 272-280.
- 693 Szydłowska-Czerniak, A., Trokowski, K., & Szłyk, E. (2011). Optimization of extraction conditions of
694 antioxidants from sunflower shells (*Helianthus annuus* L.) before and after enzymatic
695 treatment. *Industrial Crops and Products*, 33(1), 123-131.
- 696 Taha, F. S., Wagdy, S. M., Hassanein, M. M. M., & Hamed, S. F. (2012). Evaluation of the biological
697 activity of sunflower hull extracts. *Grasas y Aceites*, 63(2), 184-192.

- 698 Valdés, A., Mellinas, A. C., Ramos, M., Garrigós, M. C., & Jiménez, A. (2014). Natural additives and
699 agricultural wastes in biopolymer formulations for food packaging. *Frontiers in chemistry*, 2,
700 6.
- 701 Velioglu, Y. S., Mazza, G., Gao, L., & Oomah, B. D. (1998). Antioxidant Activity and Total Phenolics in
702 Selected Fruits, Vegetables, and Grain Products. *Journal of Agricultural and Food Chemistry*,
703 46(10), 4113-4117.
- 704 Versino, F., Lopez, O. V., Garcia, M. A., & Zaritzky, N. E. (2016). Starch-based films and food coatings:
705 An overview. *Starch - Stärke*, 68(11-12), 1026-1037.
- 706 Vilaplana, F., & Gilbert, R. G. (2010). Two-dimensional size/branch length distributions of a branched
707 polymer. *Macromolecules*, 43(17), 7321-7329.
- 708 Vilaplana, F., Hasjim, J., & Gilbert, R. G. (2012). Amylose content in starches: Toward optimal
709 definition and validating experimental methods. *Carbohydrate Polymers*, 88(1), 103-111.
- 710 Vilaplana, F., Meng, D., Hasjim, J., & Gilbert, R. G. (2014). Two-dimensional macromolecular
711 distributions reveal detailed architectural features in high-amylose starches. *Carbohydrate*
712 *Polymers*, 113, 539-551.
- 713 Wang, L., & Wang, Y. J. (2001). Structures and physicochemical properties of acid-thinned corn,
714 potato and rice starches. *Starch-Stärke*, 53(11), 570-576.
- 715 Weisz, G. M., Kammerer, D. R., & Carle, R. (2009). Identification and quantification of phenolic
716 compounds from sunflower (*Helianthus annuus* L.) kernels and shells by HPLC-DAD/ESI-MSn.
717 *Food Chemistry*, 115(2), 758-765.
718

Supplementary data

[Click here to download Supplementary data: 181127 Supplementary Figures.docx](#)